J. Biochem. 2011;149(1):103–115 doi:10.1093/jb/mvq124

JB THE JOURNAL OF BIOCHEMISTRY

Mega assemblages of oligomeric aerolysin-like toxins stabilized by toxin-associating membrane proteins

Received August 11, 2010; accepted October 8, 2010; published online October 22, 2010

Hiroyasu Shimada and Sakae Kitada*

Department of Bioscience and Bioinfomatics, Kyushu Institute of Technology, Iizuka, Fukuoka 820-8502, Japan

*Sakae Kitada, Department of Chemistry, Faculty of Sciences, Kyushu Institute of techology, Iizuka, Fukuoka 820-8502, Japan. Tel: +81 92 2948 7804, Fax: +81 92 2948 7801, email: s.kitscc@mbox.nc.kyushu-u.ac.jp

Most β pore-forming toxins need to be oligomerized *via* receptors in order to form membrane pores. Though oligomerizing toxins frequently form SDS-resistant oligomers, it was questionable whether SDS-resistant oligomers reflected native functional toxin complexes. In order to elucidate the essence of the cytocidal assemblages, oligomers of aerolysin-like toxins, aerolysin, parasporin-2 and epsilon toxin, were examined with or without SDS. On Blue Native PAGE, each toxin, which had been solubilized from target cells with mild detergent, was a much larger complex (nearly 1 MDa) than the typical SDS-resistant oligomers (~200 kDa). Size exclusion chromatography confirmed the huge toxin complexes. While a portion of the huge complexes were sensitive to proteases, SDS-resistant oligomers resist the proteolysis. Presumably the core toxin complexes remained intact while the cellular proteins were degraded. Moreover, intermediate complexes, which included no SDS-resistant oligomers, could be detected at lower temperatures. This study provides evidence for huge functional complexes of β pore-forming toxins and emphasizes their potential variance in composition.

Keywords: aerolysin/oligomer/parasporin/pore-forming toxin.

Abbreviations: ASB-1, assembly-1; ASB-2, assembly-2; BN–PAGE, Blue native PAGE; CDC, cholesterol-dependent cytolysin; Cyto, cytosol; DDM, n-dodecyl-β-D-maltoside; ETX, epsilon toxin; GAPDH, glyceraldehyde-3-phosphate dehydrogenase; GPI, glycosylphosphatidylinositol; MDCK, Madin Darby canine kidney; Mem, total membrane; PMSF, phenylmethylsulphonyl fluoride; PNS, post-nuclear supernatant; PS2, parasporin-2; TfR, transferrin receptor.

Many bacterial pathogens produce pore-forming toxins that act to increase the permeability of the plasma membrane of individual target cells (*1*, *2*). Pore-forming toxins are found in a wide range of organisms and make up at least a third of all characterized toxins. The mechanism of the cytotoxic pore formation is fundamentally common among the toxins. In the first step, the water-soluble toxins are released from the bacteria and bind to the target plasma membrane *via* receptors frequently localized in the membrane micro-domain, the lipid rafts. Next, the toxins assemble into ring-like shapes on the membrane, often called a 'prepore complex', which is believed to consist of non-toxic oligomers. Finally, the circular toxins are simultaneously inserted into the membrane, resulting in a pore in the plasma membrane (*1*, *2*). Two types of pore-forming toxins are known: the α pore-forming toxins that form a pore through an amphiphilic α helical assemblage and the β pore-forming toxins (*3–5*). In contrast to the α pore-forming toxin, the β toxin pore is thought to be constructed by an assemblage of rigid antiparallel β-sheets, which is frequently detected as a SDS-resistant oligomer by electrophoresis (*6–8*).

Aerolysin-like toxins, a new group of β pore-forming toxins including *Aeromonas hydrophila* aerolysin, *Clostridium perfringens* epsilon toxin (ETX[1]), a parasitic mushroom *Laetiporus sulphureus* haemolytic lectin, LSL, and *Bacillus thuringiensis* parasporin-2 (PS2) (*9–12*), make a SDS-resistant oligomer that is estimated to be a heptameric complex by SDS–PAGE. In spite of poor similarities between their primary structures, aerolysin-like toxins are composed of rich β-strands aligned along their long axis and include similarly folded β-sandwiches (*13*, *14*). Most recently, a crystal structure of PS2 was solved and was found to be highly similar to ETX, indicating that there may be some functional overlap (*15*). Though all toxins form SDS-resistant oligomers in plasma membranes, the target cells can be vastly different. PS2 efficiently affects human hepatoma cells whereas ETX is known to kill only Madin Darby canine kidney (MDCK) cells (*11*, *16*, *17*).

Parasporin, a new class of cry toxins from *B. thuringiensis*, was recently identified (*11*, *18–21*) and shown to exhibit cytotoxicity towards mammalian cell lines. In particular, it was clearly observed that PS2 preferentially killed human cancer cell lines (*11*, *17*). The cytotoxicity of the toxin varies considerably among different cell types. For example, it is highly cytotoxic toward HepG2 (human hepatocyte cancer) cells, but less so toward HC (human normal hepatocyte) and HeLa (human uterine cancer) cells. The toxin appears to bind specifically to lipid rafts of the plasma membrane *via* GPI-anchored proteins of susceptible cells (*22*, *23*). Subsequently, the membrane-binding toxins oligomerize into SDS-resistant

forms (*22*) resulting in a rapid increase in membrane permeability (*17*). Since PS2 is not pathogenic, unlikely other aerolysin-like toxins, PS2 would be a safe model molecule for analysing the assembly of β pore-forming toxins.

SDS-resistant protein oligomerizations have been reported for various organisms, including toxins from exogenous bacteria as described above (*6–8*, *24*, *25*) and endogenous pathogenic proteins, such as prions, amyloid β and polyglutamic huntingting found in mammalian nerve cells (*26–33*). When polypeptides enriched in β-sheets are concentrated, they strongly stack together into partly SDS-resistant forms (*30–36*). Since aerolysin-like β pore-forming toxins also accumulate in the micro domains of the plasma membrane, the physiological concentration of the acting toxins could be much higher than the concentration prior to the cytocidal action (*37*). The proteins concentrated in the intracellular compartments likely trigger the β-sheet cohesions and the oligomerizations. However, the identities of the precise oligomer compositions and formations involved in the cytocidal actions have been limited. The oligomers have been mostly analysed in the presence of denaturants.

To resolve the essence of cytocidal SDS-resistant oligomers, we examined the oligomeric assemblages of aerolysin-like toxins, including aerolysin, PS2 and ETX, with or without SDS denaturants. Under non-denaturing conditions [blue native PAGE (BN–PAGE)], all toxins assembled to much larger complexes than the typical SDS-resistant oligomers. Except for ETX, a portion of the huge complexes, likely cellular proteins, were sensitive to protease treatment, resulting in a core SDS-resistant oligomer. These huge native β pore-forming toxin complexes likely vary depending on the composition of their target membrane proteins.

Experimental Procedures

Cell culture and materials

HepG2 cells and MDCK cells were cultured in Dulbecco's modified essential medium (DMEM; Nissui) containing 10% FBS under 5% CO_2 at 37°C. PS2 was purified as described previously (*17*). The polyclonal antibody against PS2 was raised in rabbits against purified protein. Proaerolysin and the polyclonal antibody against the aerolysin were purchased from Protox Biotech (Victoria, Canada). ETX and the polyclonal antibody were gifts from Dr Sakurai and Dr Nagahama (Tokushima Bunri University). The monoclonal antibodies against glyceraldehyde-3-phosphate dehydrogenase (GAPDH), a cytoplasmic protein and transferrin receptor (TfR), a membrane protein, were purchased from HyTest and Zymed Laboratories Inc., respectively. Polyclonal antibodies against Tom40 and Tom20 were gifts from Dr Mihara (Kyushu University). Horseradish peroxidase (HRP)-conjugated secondary antibodies were obtained from Biosource (Camarillo, CA, USA). IgG from rabbit serum was obtained from SIGMA. Mixed glycosidases from *Turbo cornutus*, which contain activities of α-mannosidase, β-mannosidase, α-glucosidase, β-glucosidase, α-galactosidase, β-galactosidase, α-L-fucosidase, β-xylosidase, α-N-acetylglucosaminidase, β-N-acetylglucosaminidase, α-N-acetylgalactosaminidase and β-N-acetylgalactosaminidase, was purchased from SEIKAGAKU BIOBUSINESS CORPORATION (Tokyo, Japan). Precision Plus Protein™ Standards, a molecular weight marker of SDS–PAGE, was purchased from Bio-Rad Laboratories, Inc. and NativeMark™ Unstained Protein Standard and thyroglobulin, molecular weight markers for blue-native polyacrylamide gel electrophoresis (BN–PAGE), were purchased from Invitrogen and SIGMA, respectively.

Solubilization of toxin complex from cells

HepG2 cells (1×10^7) were treated with PS2 (1 μg/ml) or proaerolysin (1 μg/ml) at 37°C for 1 h. MDCK cells (5×10^6) were treated with ETX (1 μg/ml) at 37°C for 1 h. Then the cells were harvested and homogenized in phosphate-buffed saline [PBS; 137 mM NaCl, 8.1 mM Na_2HPO_4, 2.68 mM KCl, 1.47 mM KH_2PO_4, (pH 7.4)] by passage through a 26-gauge needle 10 times. The nuclei and cell debris were removed by centrifugation at 600*g* at 4°C for 10 min. The supernatant was centrifuged at 100,000*g* at 4°C for 30 min. The precipitate was suspended in solubilization buffer [20 mM sodium phosphate buffer (pH 7.4) containing 0.05% n-dodecyl-β-D-maltoside (DDM)] and incubated at 25°C for 1 h. After the incubation, the solubilized samples were centrifuged at 100,000*g* at 4°C for 30 min. The supernatant was used analysis for BN–PAGE.

Subcellular fractionation and toxin oligomerization

HepG2 and MDCK cells were homogenized in PBS by passage through a 26-gauge needle 10 times. The nuclei and cell debris were removed by centrifugation at 600*g* at 4°C for 10 min. The supernatant (PNS) was centrifuged at 100,000*g* at 4°C for 30 min. The supernatant and precipitate was separated as cytosol (Cyto) and total membrane (Mem) fractions. Mem was suspended in PBS, PS2 (1 μg/ml), proaerolysin (1 μg/ml) or ETX (1 μg/ml) was added in each fraction and they were incubated at 37°C for 1 h. Then, the suspensions were added to DDM (0.05% final concentration) and incubated at 25°C for 1 h followed by centrifugation at 100,000*g* at 4°C for 30 min. These supernatants including toxins were subjected to BN–PAGE and gel filtration.

BN–PAGE

The toxin complexes or monomers in solubilization buffer were subjected to BN–PAGE as described previously (*61*). Briefly, the solubilized samples were applied to a gradient polyacrylamide (3.5–16%) gel and electrophoresed under constant voltage at 4°C. After the electrophoresis, the gel was incubated with stripping buffer [62.5 mM Tris–HCl (pH 6.7) containing 100 mM 2-mercaptoethanol and 2% SDS] at 55°C for 30 min. The gel was washed and equilibrated with transfer buffer [40 mM Tris, 100 mM glycine, 20% (v/v) methanol and 0.01% SDS] at 25°C for 10 min. Proteins in the gel were transferred to a polyvinylidene difluoride membrane with transfer buffer. The membrane was blocked with PBS containing 0.05% Tween-20 and 5% skim milk, incubated with primary antibodies diluted in 20 mM Tris–HCl, pH 7.4 and 150 mM NaCl (TBS) containing 1% BSA, and then incubated with an appropriate HRP-conjugated secondary antibodies. Finally, the membranes were treated with an enhanced chemiluminescence reagent (PerkinElmer Life Sciences) and immunoreactive bands were detected using a cooled CCD camera-linked Cool Saver system (ATTO).

Size exclusion chromatography

The toxins were applied to a superose 6 10/300 GL gel filtration column (GE Healthcare) equilibrated with gel filtration buffer [20 mM sodium phosphate buffer (pH 7.4) containing 150 mM NaCl, 5% glycerol and 0.05% DDM] at room temperature. The eluate was fractionated and blotted onto a nitrocellulose membrane. The membrane was blocked with PBS containing 0.1% Tween-20 and 5% skim milk, incubated with a primary antibody diluted in 20 mM Tris–HCl (pH 7.4) containing 150 mM NaCl and 0.3% BSA, and then exposed to an appropriate HRP-conjugated secondary antibody. Finally, the membrane was reacted with an enhanced chemiluminescence reagent (PerkinElmer Life Sciences). Immunoreactive spots were detected using a cooled CCD camera-linked Cool Saver system (ATTO). Luminescence intensities were integrated and quantified by CS analyzer (ATTO).

Kinetics of PS2 oligomerization

The total membrane fraction (Mem) was prepared from HepG2 cells as described above. The Mem (500 μg proteins/ml) was incubated with PS2 (0.2 μg/ml) at 25°C or on ice for the appropriate time. After the incubation, DDM (0.1% final concentration) was added to the Mem-toxin association and incubated to solubilize. The mixture was centrifuged at 100,000*g* at 4°C for 30 min and the supernatant was subjected to SDS–PAGE and BN–PAGE. Toxin was detected with immunoblotting and the luminescence intensity was measured as described above.

Accumulation of ASB-2 and temperature-dependent ASB-1 formation

Mem (500 μg proteins/ml) was suspended in PBS and PS2 (0.2 μg/ml), proaerolysin (0.1 μg/ml) or ETX (0.1 μg/ml) was incubated with the membrane. After the incubation on ice for 60 min, toxin and membrane were centrifuged at 100,000*g* at 4°C for 30 min. The precipitate was washed twice with ice-cold PBS and suspended in ice-cold PBS. The suspension was incubated at 25°C or on ice for 60 min followed by addition to DDM for purposes of solubilizing the membrane. The suspension was centrifuged at 100,000*g* at 4°C for 30 min and the supernatant was subjected to BN–PAGE.

Treatment of toxin oligomers with proteinase K, nucleases and glycosidases

Toxin was oligomerized in Mem as described above and suspended in ice-cold PBS. During protease treatment, Proteinase K was added to the toxin-membrane and incubated on ice for 30 min. Then 1 mM phenylmethylsulphonyl fluoride (PMSF) was added to inhibit the proteolysis. One portion of the toxin-membrane suspension was run on SDS–PAGE and the rest was added to 10 times the volume of solubilization buffer for BN–PAGE. After the incubation for solubilization, the suspension was centrifuged at 100,000*g* at 4°C for 30 min, and then the supernatant was subjected to BN–PAGE. In the case of DNase and RNase treatment, the membrane suspension obtained from the toxin-treated cells was added to 1 mM $MgCl_2$ and treated with 10 μg/ml DNase I and 10 μg/ml RNase. After the incubation at 25°C for 30 min, the membrane was solubilized by DDM and analysed by SDS–PAGE and BN–PAGE as described above. For glycosidase treatment, the toxin-associated membrane was suspended in PBS and treated with mixed glycosidases (100 μg/ml) for 1 h at 37°C. DDM was added to the membrane suspension and then the divided samples were run on SDS–PAGE and BN–PAGE.

Results

Mega size complexes of aerolysin-like toxins

Aerolysin, PS2 and ETX contain multiple β-sheets with few α-helices. The structures are similar to each other in spite of their individual target specificities (Fig. 1A–C) (*13–15*). Because toxin associations with target cellular membranes induce the SDS-resistant oligomerizations, it is believed that the oligomers may be responsible for the toxin pore-formation. However, we wondered under the artificial conditions usually employed involving SDS, whether the SDS-resistant oligomers reflect intact assemblies capable of membrane pore-formation. Thus, in order to investigate oligomers of aerolysin-like toxins without

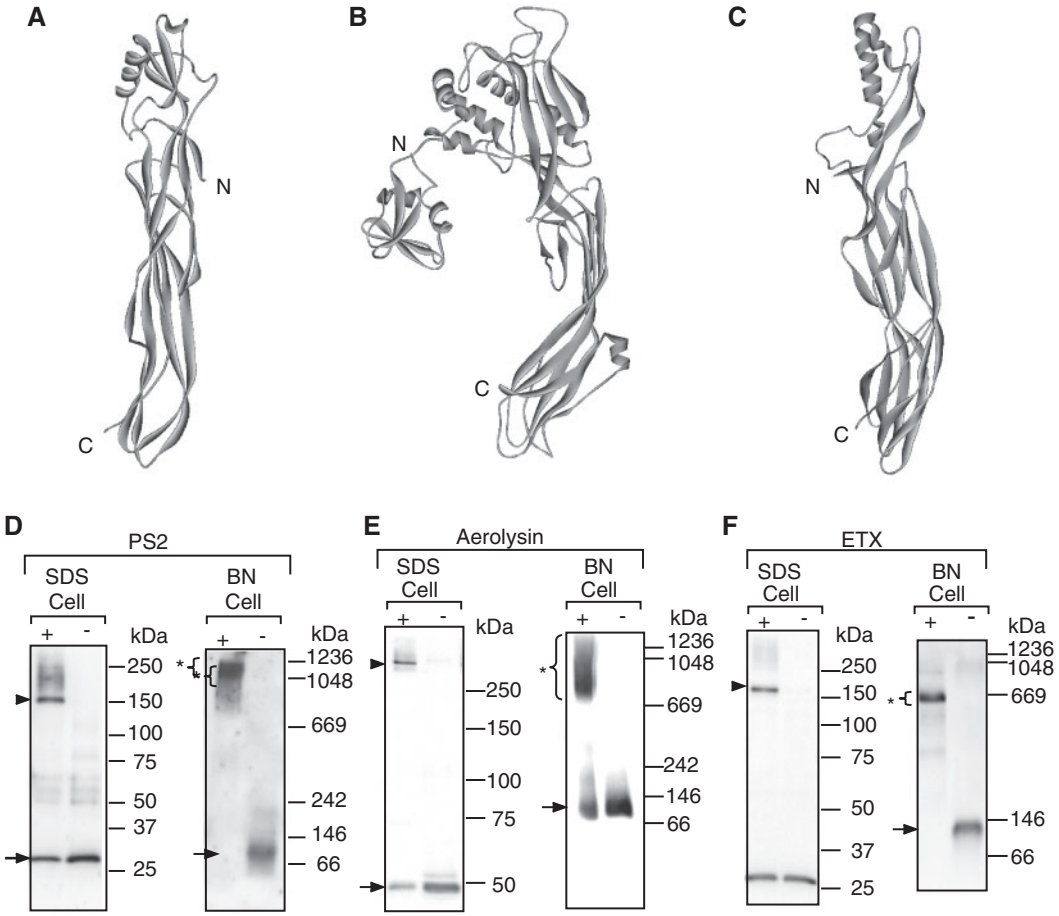

Fig. 1 Supramolecular complexes of aerolysin-like toxins under non-denaturing electrophoresis. (A–C) Ribbon models of the crystal structure of monomeric PS2 (A), proaerolysin (B) and ETX (C). N and C indicate amino and carboxyl termini, respectively (D) PS2 was incubated with or without HepG2 cells at 37°C for 1 h and homogenized. After the centrifugation of the homogenate to remove unbroken cells and nuclear material, the total membrane was solubilized by DDM. The proteins were subjected to SDS- and BN–PAGE followed by immunoblotting. (E) Oligomeric and monomeric aerolysin were prepared as described (D). Oligomeric and monomeric aerolysin were analysed by SDS–PAGE and BN–PAGE. (F) ETX was treated with or without MDCK cells. The solubilized toxins were prepared as described above and analysed by SDS–PAGE and BN–PAGE. Cell + or − indicates that same amount of each toxin was incubated with or without appropriate cells and each sample was loaded on SDS– or BN–PAGE. Arrow heads, arrows and asterisks indicate oligomeric toxins, monomeric toxins and the supramolecular complex ASB-1, respectively. Molecular weight markers are indicated for SDS–PAGE and BN–PAGE.

denaturants, toxins associated with cells were solubilized using mild detergent. After the cells were treated separately with the three toxins, the intoxicated cells were gently solubilized using n-dodecyl-β-D-maltoside (DDM) and proteins were divided and subjected to SDS–PAGE and BN–PAGE. When PS2 was analysed by SDS–PAGE and immunoblotting using anti-PS2 antibodies, it was detected as a PS2 monomer or the SDS-resistant oligomer (Fig. 1D, left panel). The migrations corresponded to ~30 and 150 kDa, respectively, the same as our previous report (*22*). Aerolysin monomer and oligomer were identified at ~45 and over 300 kDa, respectively (Fig. 1E, left panel), and ETX was found as a 30 kDa monomer and 160 kDa SDS-resistant oligomer (Fig. 1F, left panel), consistent with previous reports (*6*, *38*, *39*).

On the contrary, when aerolysin and PS2 were incubated with the cells, they migrated as distinct assemblies with a size of ~1000 kDa (1 MDa) and at least 669 kDa, corresponding to 25–40 toxin monomers on BN–PAGE (Fig. 1D and E, right panel). ETX harvested from MDCK cells was observed as condensed band at around 669 kDa on BN–PAGE (Fig. 1F, right panel), which was smaller than the PS2 and aerolysin assemblages. The mega size of toxin assemblages was a novel finding thus we defined assembly-1 (ASB-1) as huge complexes of aerolysin-like toxins formed during the cytocidal actions. ASB-1 was formed only after the toxins associated with the cells since the three toxins alone migrated on BN–PAGE as complexes of under 100 kDa, indicating at least dimers or trimers (Fig. 1D–F, right panel). Moreover, the toxins' complexes were detected as molecular mass of 150–300 kDa on BN–PAGE after they were solubilized by SDS (data not shown), indicating ASB-1 could be composed of SDS-resistant oligomers. Therefore this result clearly showed that aerolysin-like toxins associate with cells to form a mega assemblage under mild detergent conditions and BN–PAGE analysis. However, it remains unknown precise size of ASB-1 because how much micelle of lipid and detergent effect on the size of ASB-1 on the BN–PAGE analysis. In contrast, SDS-resistant toxin oligomers were much smaller complexes, owing to possible loss of some element or denaturation. These results suggest that soluble aerolysin-like toxins form supramolecular complexes, identified here as ASB-1s, which provide a new insight into the pore-forming toxin's assemblage on target cells.

ASB-1 formation required for cellular membrane

SDS-resistant oligomerizations have been shown to occur using isolated cellular membrane (*22*). To elucidate whether the ASB-1s could be assembled under a cell free system, we analysed the ASB-1 formation in the subcellular fractionated cytosol or total membrane. After post-nuclear supernatants (PNS) from the cell homogenate were isolated, PNS was centrifuged using ultrahigh speed to separate the cytosolic supernatant (Cyto) and total membrane pellet (Mem). The subcellular distributions of marker proteins were examined according to the cytoplasmic and plasma membrane proteins, GAPDH and TfR, respectively, and sufficient separations were achieved. The two fractions were then individually incubated with aerolysin-like toxins. ASB-1s appeared after incubation with the PNS and Mem whereas they were no signals after incubations with the cytosol (Fig. 2, BN). As the amount of total membrane concentrations were essentially the same for PNS and Mem, the amount of ASB-1s formed was approximately equal in either case (Fig. 2, BN). SDS-resistant oligomerization was parallel to ASB-1 formation, indicating all toxins complexed with the cellular membrane. When PS2 was incubated with solubilized membrane, no ASB-1 was formed. Instead of ASB-1, another smaller molecular weight PS2 complex was detected, indicating that ASB-1 formation required membrane but that the immature PS2 complex was formed with solubilized membrane components [Supplementary Fig. S1A (lane 1) and B (lane 3)]. ASB-1 from PS2 was not formed with membrane from HeLa cells as the cells have a low susceptibility to PS2 (Supplementary Fig. S1A, lane 3). Solubilized HeLa membrane was null for PS2-complex formation (Supplementary Fig. S1B, lane 1). Therefore, immature PS2-complex formations were specific to HepG2 membrane fractions. These results indicated that intact membrane from PS2-sensitive cells were required for ASB-1 formation. When we incubated the toxins with total membranes in the presence or absence of cytosol, the sizes and efficiencies of ASB-1 formations were essentially the same (Fig. 2, BN, +Cyto and −Cyto). Thus, appropriate membrane from each toxin target cell was sufficient for ASB-1 formation of aerolysin-like toxin.

Huge toxin complexes by size exclusion chromatography

We employed size exclusion chromatography to analyse the dependence of ASB-1 formation on the type of cellular membrane. Aerolysin-like toxins alone or the solubilized proteins from intoxicated membrane were passed though a gel filtration column, which resolved a wide range of molecular weights, resulting in the elution of fractionated proteins. The relative existence of the toxin in each fraction was assigned by immunoblotting. PS2 and aerolysin complexes eluted between the void (around 5 MDa) and thyroglobulin (669 kDa) (Fig. 3A and B, left panel). Each of them was identified as peak-1 (p1), which was estimated to be at least 669 kDa and almost 2000 kDa (Table I). Some toxins were observed in peak-2s (p2). Their molecular weights were estimated to be ~150 kDa, suggesting the presence of membrane-associated heterogeneous toxin complexes or partial dissociation of the complex units during the chromatography. Since aerolysin and PS2 alone were detected in peak-3s (p3), much smaller in molecular weight than p2s (Fig. 3A and B, right panel), the toxins in p2s were not monomers but rather were multimeric toxins. On the contrary, ETX was eluted as a single peak corresponding to 450 kDa (Fig. 3C, Table I), indicating that the toxin complex was larger than the SDS-resistant oligomer but smaller than the aerolysin and PS2 mega complexes found in p1s. These results resembled the observations of the toxin complexes on BN–PAGE where the migration of ASB-1 from ETX was around 600 kDa in contrast

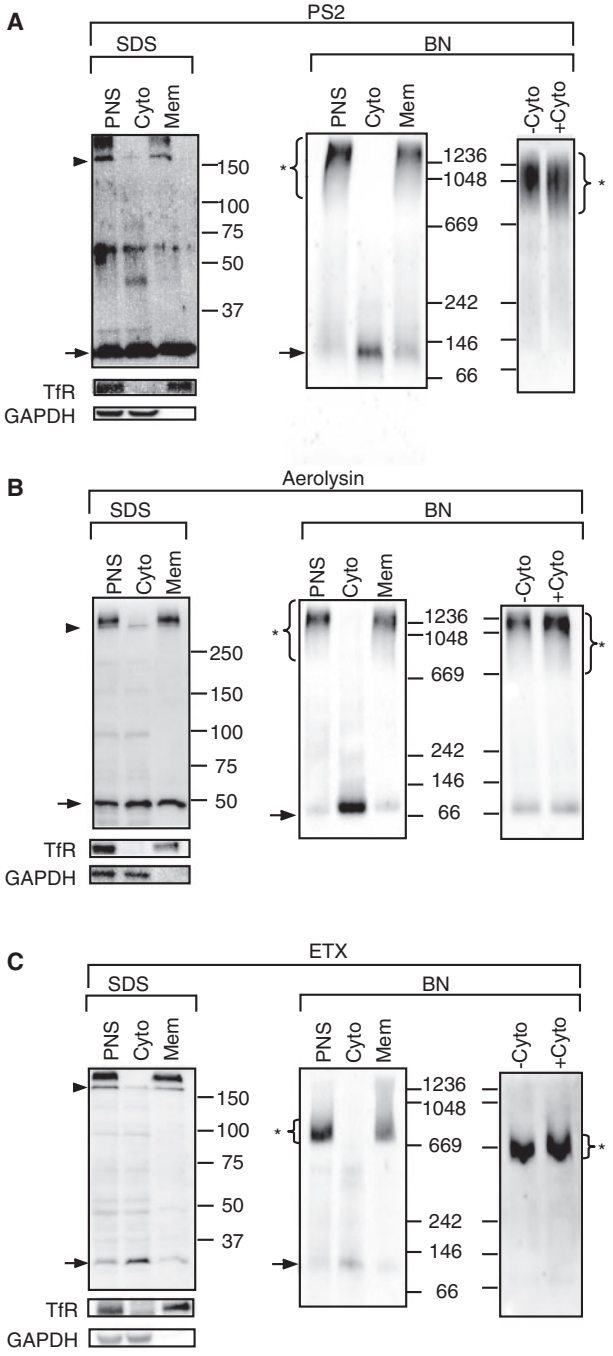

Fig. 2 Membrane-dependent ASB-1 formations of aerolysin-like toxins. (A) Post-nuclear supernatant (PNS), cytosol (Cyto) and total membrane (Mem) from HepG2 cells were fractionated as described in 'Material and Methods' section. Each fraction was incubated with PS2 and subjected to SDS–PAGE (SDS) and BN–PAGE (BN). In the right panel of BN, Mem (500 μg proteins/ml) with (+Cyto) or without (−Cyto) Cyto (500 μg proteins/ml or PBS) was incubated with PS2 and solubilized by adding DDM. The soluble proteins were analysed by BN–PAGE. (B) Proaerolysin incubated with PNS, Cyto or Mem was solubilized and subjected to SDS–PAGE and BN–PAGE. Mem (−Cyto) and the mixture of Mem and Cyto (+Cyto) was incubated with proaerolysin. Each of them was solubilized and subjected to BN–PAGE. (C) PNS, Cyto and Mem from MDCK cells were prepared, and ETX was incubated with them. After the incubation, toxins were solubilized and analysed by SDS–PAGE and BN–PAGE. ETX was incubated with Mem (−Cyto) or Mem including Cyto (+Cyto) and analysed by BN–PAGE. TfR and GAPDH are markers of membrane and cytosol protein, respectively. Toxins and marker proteins were detected by immunoblotting using appropriate antibodies. Arrow heads, arrows and asterisks indicate oligomeric toxins, monomeric toxins and the supramolecular complex ASB-1, respectively.

to the mega size ASB-1s from aerolysin and PS2. Toxin monomers were detected at ~11, 16 and 11 kDa for PS2, aerolysin and ETX, respectively (Fig. 3 and Table I). The masses of monomers estimated from the size exclusion chromatography were smaller than those from the primary sequences owing to the probable weak interactions of the toxins to the gel filtration resin. Thus, the characteristics of huge toxin assemblages observed here resemble those of ASB-1s detected on BN–PAGE.

To examine the SDS-resistant toxin in each peak obtained from gel filtration, the toxins corresponding to p1 to p3 were analysed on SDS–PAGE to determine whether they were SDS-resistant oligomers or monomeric species. While most of the p1 toxins migrated as SDS-resistant oligomers on SDS–PAGE, the p3 toxins displayed characteristic monomeric mobility. The p2s toxins of PS2 and aerolysin existed mainly as monomers with very little SDS-resistant oligomers. This suggested that p2 toxins were constructed of different toxin oligomers from the large complexes; SDS-sensitive toxin oligomers or toxins weakly associated with each other would form intermediates of ASB-1s. The p2′ of ETX seemed to contain a cross-reactive species for the anti-ETX antibody, as no signals were observed in the SDS–PAGE and immunoblot (Fig. 3D, ETX). Results from gel filtration combined with SDS–PAGE and BN–PAGE indicated that SDS-resistant oligomers were the primary component of ASB-1s.

ASB-1 formation correlated with SDS-resistant oligomerization

To elucidate the relationship between ASB-1 formation and SDS-resistant oligomerization of aerolysin-like toxins, we simultaneously examined the kinetics of ASB-1 formation and the SDS-resistant oligomerization. The mixture of PS2 incubated with cellular membrane at each time was divided: one part was run on BN–PAGE and the other part was applied to SDS–PAGE. The SDS-resistant oligomers appeared by 5 min and reached saturation by 60 min (Fig. 4A, left panel). This result was consistent with our previous kinetic analysis of the SDS-resistant emersion in HepG2 cells (*22*). The ASB-1 was slightly detected on BN–PAGE at 5 min and increased until 30 min, remaining at saturation until the analysis ended at 60 min (Fig. 4A, right panel), showing similar kinetics to the SDS-resistant oligomerization. In aerolysin or ETX, the SDS-resistant oligomerization and the ASB-1 formations of toxin were almost kinetically the same (Supplementary Fig. S2), indicating that the ASB-1s formation correlated with the SDS-resistant oligomerizations. If the SDS-resistant oligomers were an artificial complex rearranged from ASB-1, we might observe different kinetics depending on whether a potent denaturant was used (SDS–PAGE) or not (BN–PAGE). Though little is known about the relationship between the SDS-resistant oligomer and ASB-1, it is clear that the toxins associating with the cellular membrane increased ASB-1 formation.

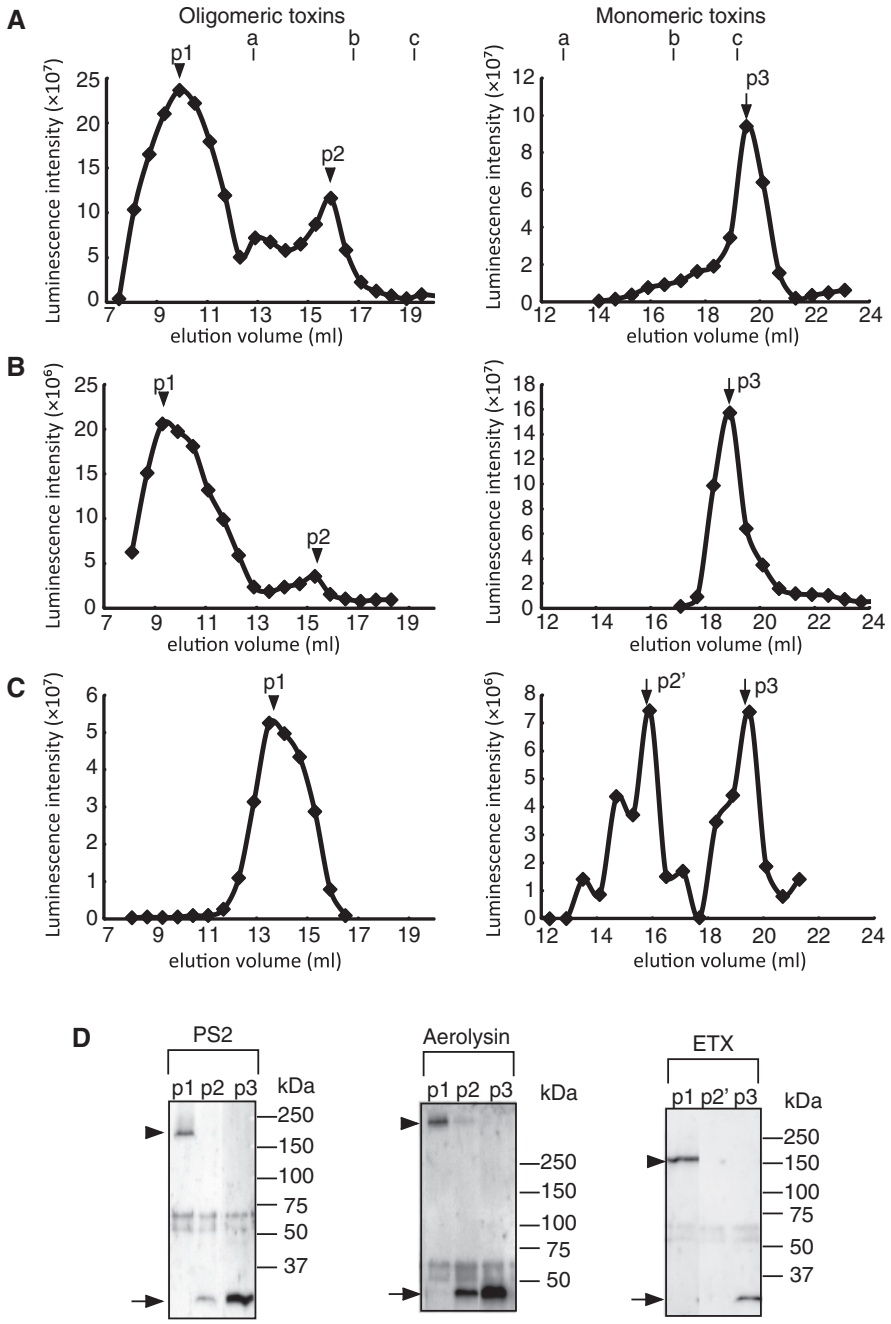

Fig. 3 Size exclusion chromatography of oligomeric and monomeric aerolysin-like toxins PS2. (A) proaerolysin (B) and ETX (C) incubated with or without Mem were solubilized and subjected to Superose 6 gel chromatography. The toxin in each eluate was analysed by spot-blotting and followed by immunoblotting as described in 'Materials and Methods' section. The vertical axis indicates intensities of the immuno-luminescence. Lines with the letters a, b and c indicates molecular weight maker proteins, thyroglobulin (669 kDa), BSA (66 kDa) and cytochrome *c* (12 kDa), respectively. (D) Fractions of P1, P2, P2′ and P3 from each toxin were subjected to SDS–PAGE and detected by immunoblotting, using anti-PS2, anti-aerolysin and anti-ETX antibodies. Arrow heads and arrows indicate oligomeric toxins and monomeric toxins, respectively.

Intermediate toxin assemblages accumulated in membrane

Prior to formation of the ASB-1, we identified another assemblage (ASB-2) with a wide range of molecular mass between 600 and 150 kDa on BN–PAGE (Fig. 4A, BN). The membrane-associated ASB-2 was much smaller than ASB-1 but obviously larger than the PS2 monomer (lane, −TM). ASB-2 was only formed in the presence of cellular membrane, suggesting that the toxin was associated with some factor(s) in the membrane. ASB-2 was observed even at the zero time incubation whereas ASB-1 was barely detected (Fig. 4A, *BN*). Since it took several minutes to recover the membrane-associated toxin by centrifugation, ASB-2 could have been formed during the chilled conditions. While ASB-1 formation was gradually increased and almost saturated between 30 and 60 min, slight reduction of smear bands of ASB-2 was observed. This incompatible stoichiometry was also observed between toxin monomer and multimer

Table I. Molecular weight of toxin complexes and monomers estimated from gel filtration chromatography.

Toxins	Oligomeric		Monomeric
	P1 (kDa)	P2[a] (kDa)	P3 (kDa)
PS2	>669 (~2000)[b]	130	11
Aerolysin	>669 (~2000)[b]	170	16
ETX	450	ND[c]	11

Molecular standard curve was constructed from the elution volume of the marker molecular, tyroglobulin (669 kDa), BSA (66 kDa), cytochrome c (12 kDa) and tryptophan (0.2 kDa). Each molecular weight of the toxin was estimated from the standard curve. [a]Minor peak, [b]Complex sizes were estimated with a molecular standard and void volume curve, [c]Toxin was not detected.

in SDS-resistant oligomerization (Fig. 4A, SDS). In spite of increase of SDS-resistant oligomer, the monomer seemed to be steady. This might depend on differences in the antibody affinity between toxin monomer and SDS-resistant oligomer. Then, we analysed the behaviour of PS2 on BN–PAGE after the toxin was incubated with chilled membrane. The results indicated that there was no ASB-1 formed and ASB-2 was accumulated between 600 and 150 kDa (Fig. 4B, BN). Moreover, ASB-2 was formed immediately after the toxin association with the cellular membrane and was maintained during long incubations. As shown by the SDS–PAGE of the toxin, SDS-resistant oligomers were reduced and instead the toxin was found as a monomer (Fig. 4B SDS). Therefore, ASB-2 consisted of a SDS-sensitive complex with an assemblage that was very different from ASB-1. The ASB-2-like complex was also observed in the presence of solubilized membrane from HepG2 cells whereas no ASB-2 was formed in the presence of HeLa cells (Supplementary Fig. S1). These results suggested that ASB-2 was a complex that consisted of PS2 and the receptor (and/or binding factors) existing on the susceptible cell membrane.

Since ASB-2 appeared earlier than ASB-1 and retained a smaller assembly than ASB-1, we suspected that ASB-2 was an intermediate of ASB-1. To further investigate the relationship between ASB-1 and -2 with the three aerolysin-like toxins, we examined whether ASB-2 that was accumulated under ice cold conditions could be subsequently converted into ASB-1 at 25°C. The results with the three toxins showed that in all three cases most of the ASB-2 was shifted to ASB-1 (Fig. 4C). The increase in the luminescence intensity of the ASB-1 that was converted from the ASB-2 was larger than the decrease in intensity of the ASB-2. This seemed to depend on differences in the antibody affinity between ASB-1 and -2. To understand composition of ASB-1 and -2, 2D PAGE analysis was performed, i.e. the first dimension to separate complex on BN–PAGE and then the second dimension to run the gel of BN–PAGE on SDS–PAGE. The results clearly showed formations of toxin assemblages. While ASB-1 was composed of SDS-resistant toxin oligomers, ASB-2 was run as monomer (Supplementary Fig. S3). In conclusion, ASB-2, which accumulated on the membrane including SDS-sensitive toxins, was related to supramolecular ASB-1 formations containing SDS-resistant toxin oligomers. Thus, ASB-2 was presumed to be an intermediate or precursor of ASB-1.

Protease-sensitive and -resistant polypeptide in ASB-1

After determining that aerolysin-like toxins initially formed the smaller ASB-2 and then converted into ASB-1 during interaction with the membranes, we were interested in the mechanism responsible for their assembly into the huge complex in the membrane. Cellular factors might bind to the toxin complex or alternatively the toxins might assemble themselves. To explore the components associated with ASB-1 of aerolysin-like toxins, we examined the hydrolytic resistances of the ASB-1 by various enzymes. When membrane-associated ASB-1 was treated with proteinase K, the SDS-resistant toxin oligomer was found to be resistant to the protolysis (Fig. 5, SDS). TfR was digested with proteinase K resulting in the cleavage of almost all the polypeptides of plasma membrane surface. The ASB-1s of PS2 and aerolysin were decreased with proteinase K treatment. Instead of the reduction of ASB-1s, however, they seemed to be reduced to a smaller assemblage ~700 kDa on BN–PAGE (Fig. 5). These results indicated that ASB-1 consisted of polypeptides that varied in their sensitivity to proteolysis. The analysis of ETX indicated that a mobility shift of ASB-1 after proteolytic treatment was not observed. Since proteinase K treatment could not degrade the SDS-resistant toxin oligomers, the oligomers were probably rigid complexes.

We investigated other possibilities of the content of ASB-1, including polynucleotides. It has been reported that *B. thuringiensis* parasporal inclusion included Cry1 toxins and heterologous 20 kb DNA fragments (*40*, *41*). Thus we analysed whether the ASB-1 of aerolysin-like toxins contained DNA or RNA. After the ASB-1s were digested by a mixture of DNase and RNase, the mobility shifts of the ASB-1s were slightly reduced on BN–PAGE (Supplementary Fig. S3A) and the SDS-resistant oligomers were not affected. The nuclease mixture efficiently digested endogenous 28S and 18S ribosomal RNA. Thus, it was likely that ASB-1 contained less polynucleotides.

It is also possible that glycans on the cell surface may play a role in the toxins binding to cells. It has been reported that aerolysin or ETX may interact with glycan in GPI-anchored proteins or glycolipids, respectively (*42*, *43*). Thus, ASB-1s were incubated with a glycosidase mixture that is capable of cleaving off most sugar chains. The behaviors of the ASB-1s were similar among the toxins in the presence or absence of the glycosidase mixture as shown by SDS–PAGE and BN–PAGE (Supplementary Fig. S3B). Less *O*-linked β-N-acetylglucosamine was detected when BSA modified with *O*-linked β-N-acetylglucosamine (O-GlcNAc-BSA) was treated with a mixture of glycosidases, indicating that ASB-1 likely does not contain glycans. The toxin assemblages analysed on different PAGEs coupled with the enzymatic hydrolysis indicated that the ASB-1s of PS2 and aerolysin were broadly

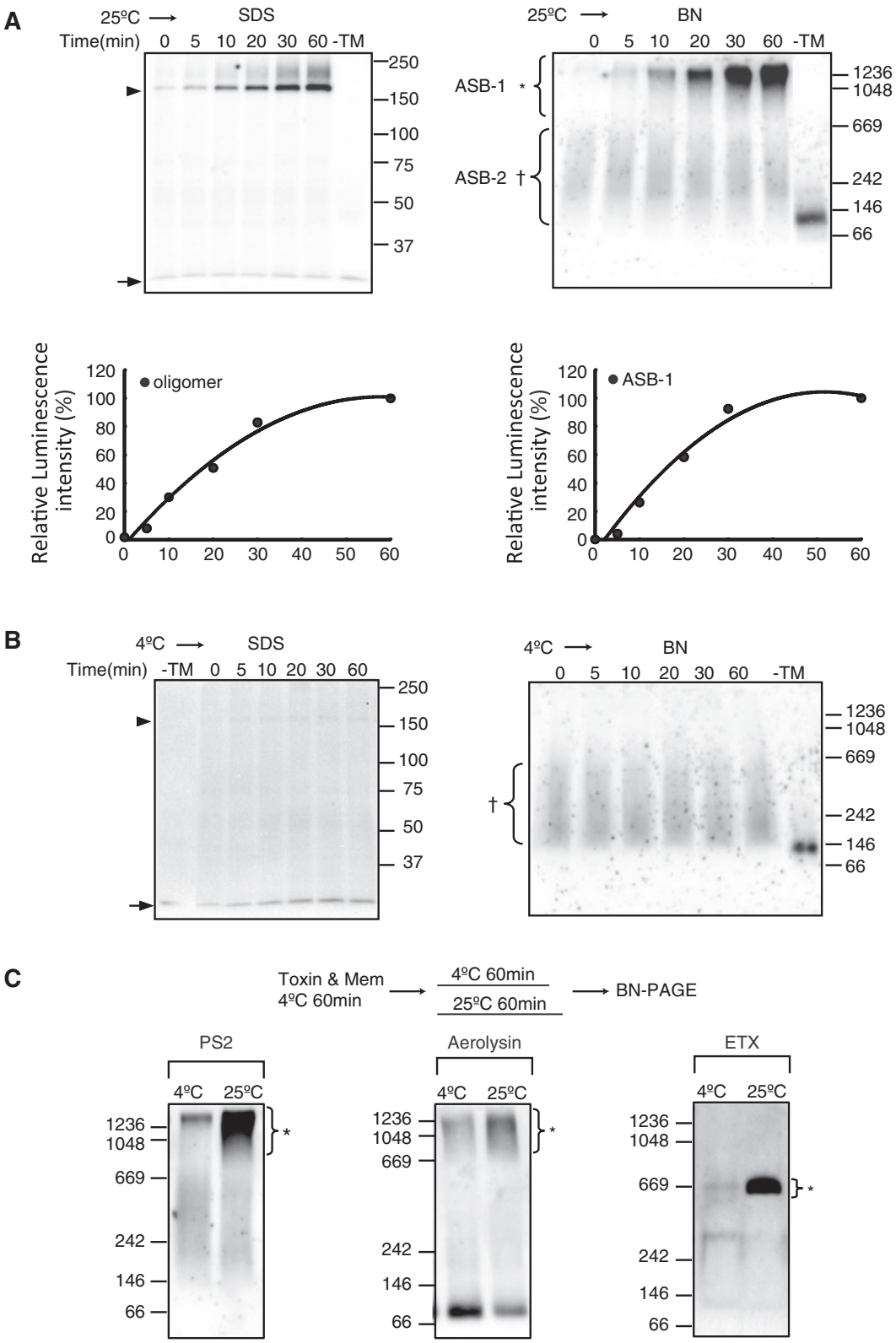

Fig. 4 Kinetics of ASB-1 and SDS-resistant oligomer formation and conversion of ASB-2 to -1. (A) PS2 was incubated with Mem from HepG2 cells at 25°C for the indicated times and added to DDM for membrane solubilization to stop toxin oligomerization. The solubilized PS2-Mem association and PS2 alone incubated at 25°C for 60 min (−TM) were subjected to SDS–PAGE (SDS) and BN–PAGE (BN). The relative intensity of the PS2 signal was quantified and the signal intensity of the oligomeric PS2 incubated with Mem for 60 min was set to 100%. The closed circle indicates the PS2 oligomer or ASB-1. (B) Mem was treated with PS2 at 4°C for the indicated times and then solubilized. The soluble Mem and PS2 incubated at 4°C for 60 min (−TM) were analysed by SDS–PAGE (SDS) and BN–PAGE (BN). Arrows, arrow heads, asterisks and crosses indicate monomeric toxin, oligomeric toxin, ASB-1 and ASB-2, respectively. (C) Toxins were incubated with Mem at 4°C for 60 min and centrifuged to remove free toxins. The precipitates were suspended in ice-cold PBS and incubated at 4 or 25°C for 60 min. The suspensions were solubilized with DDM and the soluble membrane was subjected to BN–PAGE.

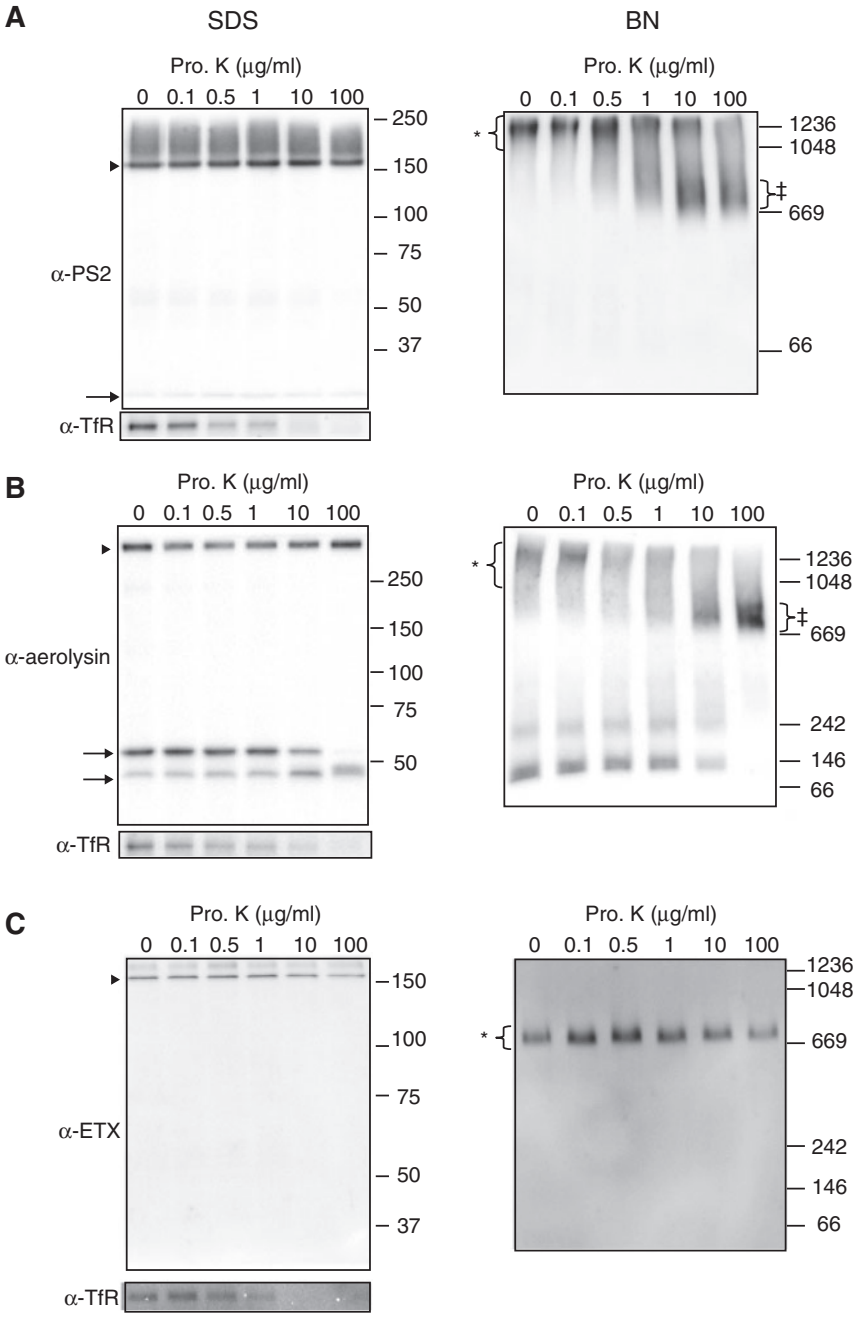

Fig. 5 Mobility shift of ASB-1 on BN–PAGE by protease treatment. (A) ASB-1 of PS2 in Mem was treated with proteinase K (Pro. K) on ice for 30 min followed by inhibition of the proteolysis by treatment with 1 mM PMSF. The soluble Mem was subjected to SDS–PAGE (SDS) and BN–PAGE (BN). (B) Mem-associated ASB-1 of aerolysin was treated by Pro. K as described in (A) and solubilized samples were analysed by SDS–PAGE (SDS) and BN–PAGE (BN). (C) Mem derived from MDCK cells was treated with ETX for ASB-1 formation, followed by proteolysis as described in (A). The solubilized Mem was run on SDS–PAGE (SDS) and BN–PAGE (BN). The Pro. K concentration is indicated for each lane. Arrow heads, arrows and asterisks indicate oligomeric toxins, monomeric toxins and the supramolecular complex ASB-1, respectively.

constituted with heterogeneous polypeptides, a proteinase K-resistant core and proteinase K-sensitive components. On the contrary, membrane-associated ETX seemed to be constructed from homogenous toxin oligomers, owing to the stability of ASB-1 under the tested hydrolytic treatments.

Discussion

Aerolysin-like toxin complexes that would exist in a nearly native state in cellular membranes were unexpectedly huge and much larger than the SDS-resistant oligomers. We defined here a novel toxin complex, ASB-1, observed on BN–PAGE as large complexes of aerolysin-like pore-forming toxins, and characterized their formations and compositions. First, formation of the ASB-1 complex required cellular membrane without cytosolic factors. Second, prior to formation of the ASB-1 complex, intermediate ASB-2 was observed and it was subsequently converted into ASB-1. Finally, the ASB-1 could be involved in some cellular membrane proteins, and

may mediate the supra-oligomerization of toxins. The ASB-1 likely reflects more the actual pore-forming complex of aerolysin-like toxins embedded in the membrane than the SDS-resistant oligomers. Therefore, SDS-resistant oligomers may be an artificial representation of β pore-forming toxins although they substantially reflect the stable association between toxins. Rather the supramolecular complex in the cellular membrane may form the cytocidal construct with involvement by cellular proteins.

Though the percentage alignment of the amino acid sequences of aerolysin-like toxins is low, they are classified into a toxin family based on similarities in protein folding and the action of their membrane pore-formation (*15*). The toxin family is now composed of four toxins from different species: aerolysin, ETX, PS2 and LSL. The N-terminal domains, which are composed of small β-sheets and short α-helices, are different in polypeptide folding patterns among the toxins, and are probably the target-binding modules (Fig. 1). Other domains include β-sandwiches, which are thought to be involved in oligomerization (*15*). While the SDS-resistant oligomers are characteristic of all of them, the precise structures of the toxin oligomers are unknown except for an aerolysin mutant of a heptameric oligomer (*44*). In our biochemical study, two toxin oligomeric states, ASB-1 and -2, were found. The ASB-1s of aerolysin and PS2 show huge complexes with sizes >1 MDa and involve target membrane proteins. Aerolysin forms complexes with proteins of various sizes including many GPI-anchored proteins that have been reported to be aerolysin receptors (*45*, *46*). The ASB-1 of ETX under 1 MDa is obviously smaller than the other two toxins. Though the ETX receptor has not been identified yet, it has been suggested that the ganglioside content may affect the binding of ETX (*43*). If ganglioside content is essential to binding of ETX, the glycolipid may be contained in the ASB-1. However, the glycosidase treatment had no impact on the ASB-1 formation. Thus, it can be concluded that the ASB-1 of ETX is constructed without receptor, or otherwise it is artificially dissociated from the ASB-1 during DDM detergent extraction or other experimental manipulations. Though the precise molecular contents of the ASB-1s are unknown, cellular factors assembled with the complex are considerable.

In addition to the ASB-1, we identified other complexes, termed ASB-2s, from aerolysin, PS2 and ETX on BN–PAGE. They appeared during the initial incubation of the toxins with the membrane or under incubation in ice cold conditions. Of note was that ASB-2 formed heterogeneously in various sizes. Once ASB-2 accumulated under lower temperatures, it was able to shift to the ASB-1 complex, suggesting that the ASB-2 was likely an immature complex and precursor of ASB-1. The toxin receptor or mediator molecule likely helped to accelerate toxin oligomerization on the membrane. The oligomer units may concentrate *via* an adaptor molecule and associate with each other in the restricted membrane domain, lipid rafts. It is also notable that the SDS-resistant oligomers are reduced in the ASB-2 (Fig. 4B) and rather rich in the ASB-1 (Fig. 4A), meaning that drastic rearrangement of interactions occurs during transition from ASB-2 to -1. Moreover, due to the absence of ASB-1 formation under ice cold conditions, membrane fluidity could be required for conversion of ASB-2 to -1. Once the membrane gains fluidity, ASB-2 seems to irreversibly change to ASB-1. Thereby, this conversion represents a key step of huge oligomerization and pore-formation of aerolysin-like toxins though our present result could not exclude direct ASB-1 formation bypassed ASB-2 intermediate. The molecular relationship between the ASB-1 and -2 should become clearer as the toxin mechanism is further elucidated.

Aerolysin-like toxins at concentrations of LD_{50} behave as a monomer or homodimer in physiological solutions. When they are concentrated by 100- or 1000-fold, they spontaneously aggregate (H. Shimada and S. Kitada, unpublished results). We regard toxin concentration by self-aggregation in solution as a key characteristic to better understanding the ASB-1 formation. When the toxins bind to receptors, they are enriched in the lipid rafts of the planer membrane. In the putative model of aerolysin-like toxins on the mode of action to the target membrane, the monomeric or dimeric toxin specifically binds to the appropriate receptor(s) localized in the lipid rafts. In the case of aerolysin and PS2, GPI-anchored proteins absolutely mediate the toxin-membrane association (*23*, *42*, *46*). In addition to GPI-anchored proteins, we assume PS2-specific receptor though it has been unidentified yet. PS2 may exhibit a narrower cytocidal spectrum due to co-receptor interaction, PS2-receptor and GPI-anchored proteins, increase of specific and high-affinity to human hepatoma cells. ETX receptor targets membrane probably *via* gangliosides that are also abundant in lipid rafts. Therefore, lipid rafts seem to provide a planar concentration of aerolysin-like toxins and the concentrated toxins are able to be oligomerized. A toxin oligomer showing SDS-resistance is likely a core unit, which is built up with multiple β-barrel strands from the heptameric interaction (*44*, *48*) and this structure is similar to pore-forming α-haemolysin (*49*). Under this hypothesis, ETX could be assembled only with a limited number of the core units because the non-denaturing complex is ∼700 kDa, which corresponds to at least four tight oligomeric units. The average masses of aerolysin and PS2 complexes reach a mega dalton. The differences in the construction between the complexes are thought to be the presence or absence of toxin-interacting proteins, receptors and cofactors, which may link the oligomeric units. Supporting this idea, we showed that most the ASB-1s of aerolysin and PS2 were digested by proteinase K to smaller complexes (∼700 kDa), sizes that are close to the ASB-1 complex of ETX. Moreover, the proteinase K-resistant complexes still exhibited SDS-resistance. One possibility is that the receptor or mediating-linker of the toxin complex is sensitive to proteinase K and that the tight oligomer resists the proteolysis, or alternatively, that immature toxins in the complex are digested by the protease. Regardless, we propose a new assembly model of aerolysin and PS2 that includes toxin-binding proteins in the cell

membrane. The toxin is first concentrated *via* a receptor in lipid rafts and rigidly oligomerized with several oligomers in one unit. Secondly, the oligomer units are attached by binding-proteins to mega assemblages. Finally, the toxin complexes form pores in the membrane resulting in target cell lysis. Though the actual step of β pore-forming toxin insertion into the membrane is unknown, it probably occurs after toxin oligomerization.

The mechanism of toxin pore-formation is primarily known for cholesterol-dependent cytolysin (CDC) from various microbes (*1*, *50*–*52*). CDCs bind to cholesterol and concentrate in a cholesterol rich domain, lipid rafts. Next about 30–50 CDC monomers form an annular structure on the membrane, called a prepore complex, and cooperatively insert the loop regions to form a β-barrel structure in the membrane (*53*). The mode of toxin membrane insertion has been revealed by real time atomic force microscopy to occur one after another like a domino cascade (*54*). Finally, the lipid bilayer inside the prepore complex is broken and subsequently a large pore is formed resulting in cell lysis. Although much is known about the mechanism, the way in which CDCs exclude membrane lipids in the closed prepore complex is still not clear. The lipid exclusion from the prepore complex is a common characteristic of β pore-forming toxins. While pore sizes of CDCs are >20 nm in diameter (*53*, *55*), aerolysin-like toxin are much smaller. They are estimated to be around 2, 3 and 2 nm for aerolysin (*13*), PS2 (*17*) and ETX (*56*), respectively, by the oligomer structure of aerolysin and inhibition of membrane permeability for PS2 and ETX using various sizes of polyethylene glycols. If one unit of heptameric toxin constitutes a stable pore-forming oligomer, the tiny pores may be reasonable compared to the large pore formed by a CDC multimer. Moreover, as aerolysin-like toxins are clustered with cellular proteins, the pore-formation coupled with lipid exclusion would be complicated. Further work is required to understand the mechanism of lipid exclusion and pore-formation into the membrane.

The dangers of cytotoxic β oligomers are not only from bacterial toxins but also from the mammals themselves. The SDS-resistant β oligomers of amyloidal polypeptides are endogenously produced and sometimes show neurotoxicity. A biochemical hallmark of Alzheimer's disease is the accumulation of insoluble aggregates containing the amyloid-β peptide (Aβ) consisting of 40–42 amino acid residues. Protofibrils, key neurotoxic intermediates in synaptic dysfunction, have recently been recognized to be a soluble amyloid-β oligomer that shows SDS-resistance to oligomerization (*26*). The infectious prion protein (PrP^{Sc}) also shows PrP^{Sc} multimeric oligomers on SDS–PAGE (*27*). A common structural characteristic is the formation of β-sheet-rich polypeptides that irreversibly stack together to form protofibrils to fibrils under appropriate conditions *in vitro* and also *in vivo*. Notably, electron microscopic analysis of a mutant $Aβ_{ARC}$ oligomer fractionated from soluble protofibrils was shown to be mainly annular species with inner diameters of 1.52–2.0 nm (*57*). Moreover, a soluble Aβ oligomer has been reported to form an ion channel directly in the membrane (*58*). These reports suggest that the Aβ oligomers are able to form membrane pores. The molecular mass of oligomeric $Aβ_{ARC}$ was estimated to be 150–250 kDa, corresponding to between 40 and 60 $Aβ_{ARC}$ molecules. Moreover, Kayed *et al.* (*59*) reported that various types of soluble amyloid oligomers have common structures and they suggested that Aβ oligomers share a common mechanism of toxicity. The common cytotoxicity of the soluble Aβ oligomers has been shown to increase lipid bilayer permeability (*60*). Here we propose that the properties and cytotoxicity of Aβ oligomers resemble bacterial β pore-forming toxins. They both form annular oligomers containing 7- to 50-mer polypeptides and they integrate into membranes with increases in membrane permeability, resulting in cellular dysfunction. This common mechanism likely can explain the cytocidal effects of β oligomeric polypeptides from bacteria to mammals. Expansions in the principles of β oligomer toxicity may contribute to the development of innovative medical applications.

Supplementary Data

Supplementary Data are available at *JB* Online.

Conflict of interest
None declared.

Acknowledgements

We thank Dr Jun Sakurai and Masahiro Nagahama for the gifts of ETX and the antibody, Dr Naotada Ishihara for help with the BN-PAGE technique, and Dr Osamu Kuge, Tadashi Ogishima and Yuichi Abe for helpful discussions. This work was supported by a Grant-in-Aid for JSPS Fellows from the Japan Society for the Promotion of Science (to H.S.) and also supported in part by Grants-in-Aid for Scientific Research (to S.K./18687007) from the Ministry of Education, Science, Sports and Culture of the Japanese Government, Grants-in-Aid for Research (to S.K./08A02203a) from the New Energy and Industrial Technology Development Organization (NEDO), and the Takeda Science Foundation (to S.K.).

References

1. Gilbert, R.J. (2002) Inactivation and activity of cholesterol-dependent cytolysins: what structural studies tell us. *Cell Mol. Life Sci.* **59**, 832–844
2. Parker, M.W. and Feil, S.C. (2005) Pore-forming protein toxins: from structure to function. *Prog. Biophys. Mol. Biol.* **88**, 91–142
3. Heuck, A.P., Tweten, R.K., and Johnson, A.E. (2001) Beta-barrel pore-forming toxins: intriguing dimorphic proteins. *Biochemistry* **40**, 9065–9073
4. Gonzalez, M.R., Bischofberger, M., Pernot, L., van der Goot, F.G., and Freche, B. (2008) Bacterial pore-forming toxins: the (w)hole story? *Cell Mol. Life Sci.* **65**, 493–507
5. Iacovache, I., van der Goot, F.G., and Pernot, L. (2008) Pore formation: an ancient yet complex form of attack. *Biochim. Biophys. Acta* **1778**, 1611–1623
6. Petit, L., Gibert, M., Gillet, D., Laurent-Winter, C., Boquet, P., and Popoff, M.R. (1997) *Clostridium perfringens* epsilon-toxin acts on MDCK cells by forming a large membrane complex. *J. Bacteriol.* **179**, 6480–6487

7. van der Goot, F.G., Pattus, F., Parker, M., and Buckley, J.T. (1994) *Toxicology* **87**, 19–28
8. Miller, C.J., Elliott, J.L., and Collier, R.J. (1999) Anthrax protective antigen: prepore-to-pore conversion. *Biochemistry* **38**, 10432–10441
9. Hunter, S.E., Clarke, I.N., Kelly, D.C., and Titball, R.W. (1992) Cloning and nucleotide sequencing of the Clostridium perfringens epsilon-toxin gene and its expression in Escherichia coli. *Infect. Immun.* **60**, 102–110
10. Tateno, H. and Goldstein, I.J. (2003) Molecular cloning, expression, and characterization of novel hemolytic lectins from the mushroom Laetiporus sulphureus, which show homology to bacterial toxins. *J. Biol. Chem.* **278**, 40455–40463
11. Ito, A., Sasaguri, Y., Kitada, S., Kusaka, Y., Kuwano, K., Masutomi, K., Mizuki, E., Akao, T., and Ohba, M. (2004) A *Bacillus thuringiensis* crystal protein with selective cytocidal action to human cells. *J. Biol. Chem.* **279**, 21282–21286
12. Howard, S.P. and Buckley, J.T. (1986) Molecular cloning and expression in Escherichia coli of the structural gene for the hemolytic toxin aerolysin from Aeromonas hydrophila. *Mol. Gen. Genet.* **204**, 289–295
13. Parker, M.W., Buckley, J.T., Postma, J.P., Tucker, A.D., Leonard, K., Pattus, F., and Tsernoglou, D. (1994) Structure of the Aeromonas toxin proaerolysin in its water-soluble and membrane-channel states. *Nature* **367**, 292–295
14. Cole, A.R., Gibert, M., Popoff, M., Moss, D.S., Titball, R.W., and Basak, A.K. (2004) *Clostridium perfringens* epsilon-toxin shows structural similarity to the pore-forming toxin aerolysin. *Nat. Struct. Mol. Biol.* **11**, 797–798
15. Akiba, T., Abe, Y., Kitada, S., Kusaka, Y., Ito, A., Ichimatsu, T., Katayama, H., Akao, T., Higuchi, K., Mizuki, E., Ohba, M., Kanai, R., and Harata, K. (2009) Crystal Structure of the Parasporin-2 *Bacillus thuringiensis* Toxin That Recognizes Cancer Cells. *J. Mol. Biol.* **386**, 121–133
16. Payne, D.W., Williamson, E.D., Havard, H., Modi, N., and Brown, J. (1994) Evaluation of a new cytotoxicity assay for Clostridium perfringens type D epsilon toxin. *FEMS Microbiol. Lett.* **116**, 161–167
17. Kitada, S., Abe, Y., Shimada, H., Kusaka, Y., Matsuo, Y., Katayama, H., Okumura, S., Akao, T., Mizuki, E., Kuge, O., Sasaguri, Y., Ohba, M., and Ito, A. (2006) Cytocidal actions of parasporin-2, an anti-tumor crystal toxin from *Bacillus thuringiensis*. *J. Biol. Chem.* **281**, 26350–26360
18. Katayama, H., Yokota, H., Akao, T., Nakamura, O., Ohba, M., Mekada, E., and Mizuki, E. (2005) Parasporin-1, a novel cytotoxic protein to human cells from non-insecticidal parasporal inclusions of *Bacillus thuringiensis*. *J. Biochem.* **137**, 17–25
19. Saitoh, H., Okumura, S., Ishikawa, T., Akao, T., Mizuki, E., and Ohba, M. (2006) Investigation of a novel *Bacillus thuringiensis* gene encoding a parasporal protein, parasporin-4, that preferentially kills human leukemic T cells. *Biosci. Biotechnol. Biochem.* **70**, 2935–2941
20. Yamashita, S., Katayama, H., Saitoh, H., Akao, T., Park, Y.S., Mizuki, E., Ohba, M., and Ito, A. (2005) Typical three-domain cry proteins of *Bacillus thuringiensis* strain A1462 exhibit cytocidal activity on limited human cancer cells. *J. Biochem.* **138**, 663–672
21. Ohba, M., Mizuki, E., and Uemori, A. (2009) Parasporin, a new anticancer protein group from Bacillus thuringiensis. *Anticancer Res.* **29**, 427–433
22. Abe, Y., Shimada, H., and Kitada, S. (2008) Raft-targeting and Oligomerization of Parasporin-2, a *Bacillus thuringiensis* Crystal Protein with Anti-Tumour Activity. *J. Biochem.* **143**, 269–275
23. Kitada, S., Abe, Y., Maeda, T., and Shimada, H. (2009) Parasporin-2 requires GPI-anchored proteins for the efficient cytocidal action to human hepatoma cells. *Toxicology* **264**, 80–88
24. Bhakdi, S. and Tranum-Jensen, J. (1991) Alpha-toxin of Staphylococcus aureus. *Microbiol. Rev.* **55**, 733–751
25. Alouf, J.E. (2000) Cholesterol-binding cytolytic protein toxins. *Int. J. Med. Microbiol.* **290**, 351–356
26. Walsh, D.M., Klyubin, I., Fadeeva, J.V., Cullen, W.K., Anwyl, R., Wolfe, M.S., Rowan, M.J., and Selkoe, D.J. (2002) Naturally secreted oligomers of amyloid beta protein potently inhibit hippocampal long-term potentiation in vivo. *Nature* **416**, 535–539
27. Sindi, S.S. and Serio, T.R. (2009) Prion dynamics and the quest for the genetic determinant in protein-only inheritance. *Curr. Opin. Microbiol.* **12**, 623–630
28. Scherzinger, E., Lurz, R., Turmaine, M., Mangiarini, L., Hollenbach, B., Hasenbank, R., Bates, G.P., Davies, S.W., Lehrach, H., and Wanker, E.E. (1997) Huntingtin-encoded polyglutamine expansions form amyloid-like protein aggregates in vitro and in vivo. *Cell* **90**, 549–558
29. Fink, A.L. (2006) The aggregation and fibrillation of alpha-synuclein. *Acc. Chem. Res.* **39**, 628–634
30. Zheng, J., Jang, H., Ma, B., Tsai, C.J., and Nussinov, R. (2007) Modeling the Alzheimer Abeta17-42 fibril architecture: tight intermolecular sheet-sheet association and intramolecular hydrated cavities. *Biophys. J.* **93**, 3046–3057
31. Collinge, J. (2001) Prion diseases of humans and animals: their causes and molecular basis. *Annu. Rev. Neurosci.* **24**, 519–550
32. Pan, K.M., Baldwin, M., Nguyen, J., Gasset, M., Serban, A., Groth, D., Mehlhorn, I., Huang, Z., Fletterick, R.J., Cohen, F.E., and Prusiner, S.B. (1993) Conversion of alpha-helices into beta-sheets features in the formation of the scrapie prion proteins. *Proc. Natl Acad. Sci. USA* **90**, 10962–10966
33. Serpell, L.C. (2000) Alzheimer's amyloid fibrils: structure and assembly. *Biochim. Biophys. Acta* **1502**, 16–30
34. DiFiglia, M., Sapp, E., Chase, K.O., Davies, S.W., Bates, G.P., Vonsattel, J.P., and Aronin, N. (1997) Aggregation of huntingtin in neuronal intranuclear inclusions and dystrophic neurites in brain. *Science* **277**, 1990–1993
35. MacDonald, M.E., Ambrose, C.M., Duyao, M.P., Myers, R.H., Lin, C., Srinidhi, L., Barnes, G., Taylor, S.A., James, M., Groot, N., MacFarlane, H., Jenkins, B., Anderson, M.A., Wexler, N.S., Gusella, J.F., Bates, G.P., Baxendale, S., Hummerich, H., Kirby, S., North, M., Youngman, S., Mott, R., Zehetner, G., Sedlacek, Z., Poustka, A., Frischauf, A.-M., Lehrach, H., Buckler, A.J., Church, D., Doucette-Stamm, L., O'Donovan, M.C., Riba-Ramirez, L., Shah, M., Stanton, V.P., Strobel, S.A., Draths, K.M., Wales, J.L., Dervan, P., Housman, D.E., Altherr, M., Shiang, R., Thompson, L., Fielder, T., Wasmuth, J.J., Tagle, D., Valdes, J., Elmer, L., Allard, M., Castilla, L., Swaroop, M., Blanchard, K., Collins, F.S., Snell, R., Holloway, T., Gillespie, K., Datson, N., Shaw, D., and Harper, P.S. (1993) A novel gene containing a trinucleotide repeat that is expanded and unstable on Huntington's disease chromosomes. *Cell* **72**, 971–983
36. Gutekunst, C.A., Li, S.H., Yi, H., Mulroy, J.S., Kuemmerle, S., Jones, R., Rye, D., Ferrante, R. J., Hersch, S.M., and Li, X.J. (1999) Nuclear and neuropil

aggregates in Huntington's disease: relationship to neuropathology. *J. Neurosci.* **19**, 2522–2534
37. Abrami, L. and van Der Goot, F.G. (1999) Plasma membrane microdomains act as concentration platforms to facilitate intoxication by aerolysin. *J. Cell Biol* **147**, 175–184
38. van der Goot, F.G., Pattus, F., Wong, K.R., and Buckley, J.T. (1993) Oligomerization of the channel-forming toxin aerolysin precedes insertion into lipid bilayers. *Biochemistry* **32**, 2636–2642
39. Nagahama, M., Hara, H., Fernandez-Miyakawa, M., Itohayashi, Y., and Sakurai, J. (2006) Oligomerization of *Clostridium perfringens* epsilon-toxin is dependent upon membrane fluidity in liposomes. *Biochemistry* **45**, 296–302
40. Bietlot, H.P., Schernthaner, J.P., Milne, R.E., Clairmont, F.R., Bhella, R.S., and Kaplan, H. (1993) Evidence that the CryIA crystal protein from Bacillus thuringiensis is associated with DNA. *J. Biol. Chem.* **268**, 8240–8245
41. Xia, L., Sun, Y., Ding, X., Fu, Z., Mo, X., Zhang, H., and Yuan, Z. (2005) Identification of cry-type genes on 20-kb DNA associated with Cry1 crystal proteins from Bacillus thuringiensis. *Curr. Microbiol.* **51**, 53–58
42. Abrami, L., Velluz, M.C., Hong, Y., Ohishi, K., Mehlert, A., Ferguson, M., Kinoshita, T., and Gisou van der Goot, F. (2002) The glycan core of GPI-anchored proteins modulates aerolysin binding but is not sufficient: the polypeptide moiety is required for the toxin-receptor interaction. *FEBS Lett.* **512**, 249–254
43. Shimamoto, S., Tamai, E., Matsushita, O., Minami, J., Okabe, A., and Miyata, S. (2005) Changes in ganglioside content affect the binding of *Clostridium perfringens* epsilon-toxin to detergent-resistant membranes of Madin-Darby canine kidney cells. *Microbiol. Immunol.* **49**, 245–253
44. Tsitrin, Y., Morton, C.J., el-Bez, C., Paumard, P., Velluz, M.C., Adrian, M., Dubochet, J., Parker, M.W., Lanzavecchia, S., and van der Goot, F.G. (2002) Conversion of a transmembrane to a water-soluble protein complex by a single point mutation. *Nat. Struct. Biol.* **9**, 729–733
45. Diep, D.B., Nelson, K.L., Raja, S.M., Pleshak, E.N., and Buckley, J.T. (1998) Glycosylphosphatidylinositol anchors of membrane glycoproteins are binding determinants for the channel-forming toxin aerolysin. *J. Biol. Chem.* **273**, 2355–2360
46. Abrami, L., Fivaz, M., Glauser, P.E., Parton, R.G., and van der Goot, F.G. (1998) A pore-forming toxin interacts with a GPI-anchored protein and causes vacuolation of the endoplasmic reticulum. *J. Cell Biol* **140**, 525–540
47. Miyata, S., Minami, J., Tamai, E., Matsushita, O., Shimamoto, S., and Okabe, A. (2002) Clostridium perfringens epsilon-toxin forms a heptameric pore within the detergent-insoluble microdomains of Madin-Darby canine kidney cells and rat synaptosomes. *J. Biol. Chem.* **277**, 39463–39468
48. Song, L., Hobaugh, M.R., Shustak, C., Cheley, S., Bayley, H., and Gouaux, J.E. (1996) Structure of staphylococcal alpha-hemolysin, a heptameric transmembrane pore. *Science* **274**, 1859–1866
49. Tweten, R.K. (2005) Cholesterol-dependent cytolysins, a family of versatile pore-forming toxins. *Infect. Immun.* **73**, 6199–6209
50. Palmer, M. (2001) The family of thiol-activated, cholesterol-binding cytolysins. *Toxicon* **39**, 1681–1689
51. Gilbert, R.J. (2005) Inactivation and activity of cholesterol-dependent cytolysins: what structural studies tell us. *Structure* **13**, 1097–1106
52. Tilley, S.J., Orlova, E.V., Gilbert, R.J., Andrew, P.W., and Saibil, H.R. (2005) tructural basis of pore formation by the bacterial toxin pneumolysin. *Cell* **121**, 247–256
53. Czajkowsky, D.M., Hotze, E.M., Shao, Z., and Tweten, R.K. (2004) Vertical collapse of a cytolysin prepore moves its transmembrane beta-hairpins to the membrane. *EMBO J.* **23**, 3206–3215
54. Olofsson, A., Hebert, H., and Thelestam, M. (1993) The projection structure of perfringolysin O (Clostridium perfringens theta-toxin). *FEBS Lett.* **319**, 125–127
55. Petit, L., Maier, E., Gibert, M., Popoff, M.R., and Benz, R. (2001) J. *Biol. Chem.* **276**, 15736–15740
56. Lashuel, H.A., Hartley, D., Petre, B.M., Walz, T., and Lansbury, P.T. Jr (2002) Neurodegenerative disease: amyloid pores from pathogenic mutations. *Nature* **418**, 291
57. Demuro, A., Mina, E., Kayed, R., Milton, S.C., Parker, I., and Glabe, C.G. (2005) Calcium dysregulation and membrane disruption as a ubiquitous neurotoxic mechanism of soluble amyloid oligomers. *J. Biol. Chem.* **280**, 17294–17300
58. Kayed, R., Head, E., Thompson, J.L., McIntire, T.M., Milton, S.C., Cotman, C.W., and Glabe, C.G. (2003) Common structure of soluble amyloid oligomers implies common mechanism of pathogenesis. *Science* **300**, 486–489
59. Kayed, R., Sokolov, Y., Edmonds, B., McIntire, T.M., Milton, S.C., Hall, J.E., and Glabe, C.G. (2004) Permeabilization of lipid bilayers is a common conformation-dependent activity of soluble amyloid oligomers in protein misfolding diseases. *J. Biol. Chem.* **279**, 46363–46366
60. Nijtmans, L.G., Henderson, N.S., and Holt, I.J. (2002) Blue Native electrophoresis to study mitochondrial and other protein complexes. *Methods* **26**, 327–334